LETTERS

Imaging the biogenesis of individual HIV-1 virions in live cells

Nolwenn Jouvenet[1,2], Paul D. Bieniasz[1,2] & Sanford M. Simon[3]

Observations of individual virions in live cells have led to the characterization of their attachment, entry and intracellular transport[1]. However, the assembly of individual virions has never been observed in real time. Insights into this process have come primarily from biochemical analyses of populations of virions or from microscopic studies of fixed infected cells. Thus, some assembly properties, such as kinetics and location, are either unknown or controversial[2–5]. Here we describe quantitatively the genesis of individual virions in real time, from initiation of assembly to budding and release. We studied fluorescently tagged derivatives of Gag, the major structural component of HIV-1—which is sufficient to drive the assembly of virus-like particles[6]—with the use of fluorescence resonance energy transfer, fluorescence recovery after photobleaching and total-internal-reflection fluorescent microscopy in living cells. Virions appeared individually at the plasma membrane, their assembly rate accelerated as Gag protein accumulated in cells, and typically 5–6 min was required to complete the assembly of a single virion. These approaches allow a previously unobserved view of the genesis of individual virions and the determination of parameters of viral assembly that are inaccessible with conventional techniques.

We monitored HeLa cells coexpressing untagged Gag and Gag fused to green fluorescent protein (GFP). This avoids the reported morphological defect seen when Gag–GFP is expressed alone[7], and electron microscopic studies confirmed that virus-like particles (VLPs) containing Gag and Gag–GFP were morphologically indistinguishable from VLPs containing Gag only (data not shown). Gag was detected as a diffuse signal at 5–6 h after transfection and discrete puncta that apparently localized at the plasma membrane began to appear at 6–7 h after transfection (Supplementary Fig. 1a)[4]. However, the signal from puncta at the plasma membrane was partly masked by the strong diffuse fluorescence emitted by cytoplasmic Gag–GFP (Supplementary Fig. 1b). This diffuse fluorescence diminished relative to the intensity of the fluorescent puncta when imaged with total-internal-reflection fluorescent microscopy (TIR-FM), whose illumination decays exponentially from the coverslip/medium interface with a space constant of about 70 nm (ref. 8) (Supplementary Fig. 1b). Thus, TIR-FM is well suited to monitor the appearance of VLPs at the plasma membrane.

Cells that had generated few (less than 20) Gag puncta at 5–6 h after transfection were observed over the ensuing 30–60 min (Supplementary Fig. 1c). Typically, 50–150 puncta per cell appeared during this period (Supplementary Movie 1). Their behaviour fell into two discrete classes. One class appeared over several minutes (Fig. 1a, top, Fig. 1b, left, and Supplementary Movie 2) and showed little lateral movement during and after emergence (average lateral velocity 0.007 $\mu m\,s^{-1}$, $n = 25$, Supplementary Fig. 2a). Almost all (99%) of these slowly appearing puncta remained in the TIR field until the end of the imaging period. A second class of Gag puncta behaved differently, emerging in the TIR field in 5–15 s, remaining there for an average of 33 s ($n = 25$), displaying lateral motility (average velocity 0.195 $\mu m\,s^{-1}$, $n = 25$), and, in every case, disappearing

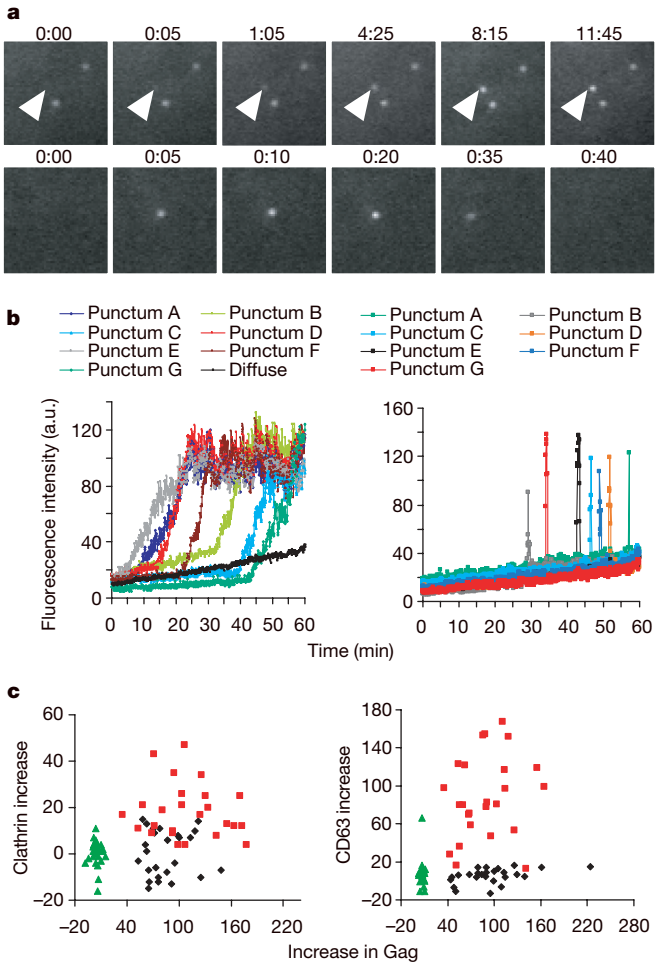

Figure 1 | Two distinct behaviours of HIV-1 Gag puncta at the plasma membrane. a, Images illustrating slowly (top panels, arrowheads) and rapidly (bottom panels) appearing Gag–GFP puncta. Fields are 5.5 μm × 5.5 μm. Numbers above the fields are minutes:seconds. **b**, Fluorescence intensity in arbitrary units (a.u.) plotted over time for seven slowly appearing puncta (left, coloured lines), for seven rapidly appearing puncta (right) and for seven random areas where no puncta appeared (left, black line). **c**, The change in clathrin (left) or CD63 (right) fluorescence is plotted against the corresponding change in Gag–GFP during the appearance of 25 rapidly emerging (red squares) and slowly emerging (black diamonds) puncta, as well as against the corresponding changes at random areas where no puncta appeared (green triangles).

[1]Aaron Diamond AIDS Research Center, [2]Laboratory of Retrovirology, and [3]Laboratory of Cellular Biophysics, The Rockefeller University, New York, New York 10065, USA.

from the field as rapidly as they appeared (Fig. 1a, bottom, Fig. 1b, right, and Supplementary Movie 3). When the Gag–GFP puncta first appeared (5–6 h after transfection), slowly appearing puncta represented the majority of events (74%, $n = 306$), whereas at later time points (14–15 h after transfection), the rapidly appearing/disappearing population predominated (75%, $n = 166$) (Supplementary Fig. 2b). When Gag was co-expressed with the viral protein Vpu, which reduces the surface tethering of virions and their subsequent appearance in late endosomes[9–11], the fraction of rapidly appearing/disappearing puncta fell both at early (from 26% to 3%) and late (from 75% to 34%; $P < 0.001$) time points (Supplementary Fig. 2b).

Virions can appear in late endosomes as a result of active antiviral tethering[9–11] and subsequent internalization[4,9–12]. Further, endosomes marked with fluorescently tagged versions of resident proteins, such as CD63 (ref. 13), or coat proteins, such as clathrin[14,15], have previously been observed moving in the TIR field. To examine whether the Gag puncta were associated with endosomes, Gag–GFP together with CD63–mCherry or with DsRed–clathrin light chain were detected with simultaneous dual-colour TIR-FM (Supplementary Movie 4). Most of the rapidly appearing/disappearing, laterally motile Gag puncta were positive for CD63 (88%, $n = 25$) and clathrin (72%, $n = 25$). The appearance, movement and disappearance of these puncta were indistinguishable from the CD63-positive or clathrin-positive vesicles (Supplementary Fig. 3a and Supplementary Movies 5 and 6). On average, the fluorescence of CD63 and clathrin increased 16-fold and 50-fold, respectively, coincident with the rapidly appearing Gag puncta, in comparison with randomly chosen, equivalently sized areas of observation containing only diffuse Gag ($P < 0.001$) (Fig. 1c). In contrast, none of the slowly appearing puncta were associated with a detectable increase in CD63 ($n = 25$) or clathrin ($n = 25$), and in this respect they were indistinguishable from areas of the plasma membrane containing only diffuse Gag ($P = 0.43$ and 0.98, respectively) (Supplementary Fig. 3b and Supplementary Movies 7 and 8). Because the rapidly appearing/disappearing puncta were indistinguishable from endosomes, we focused on the slowly appearing puncta as the population that might represent genuine VLP assembly events.

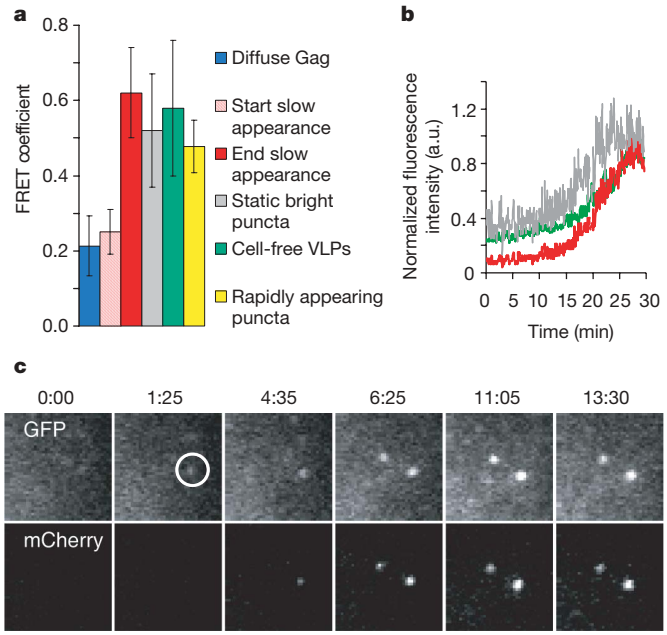

Figure 2 | FRET analysis of individual Gag puncta. Untagged Gag, Gag–mCherry and Gag–GFP were co-expressed and the cells were illuminated with a 488-nm laser. **a**, FRET coefficients measured at the beginning and the end of the slow appearance of individual puncta ($n = 30$), compared with FRET coefficients at randomly chosen areas containing diffuse Gag ($n = 30$), in static bright puncta ($n = 30$), in cell-free VLPs ($n = 100$) or in rapidly appearing puncta ($n = 30$). Errors are s.d. **b**, Plots of the normalized fluorescence intensity of GFP (green), corrected mCherry (red) and the FRET coefficient (grey) during the appearance of the punctum shown in **c**. Additional examples are shown in Supplementary Fig. 5. **c**, Images of GFP and corrected mCherry fluorescence (due to FRET) during the slow appearance of a punctum. Fields are 5.5 μm × 5.5 μm. Numbers above the fields are minutes:seconds.

During virion assembly, Gag molecules become sufficiently close to one another that FRET can occur. Indeed, fluorescence resonance energy transfer (FRET) has been demonstrated between retroviral Gag–cyan fluorescent protein (CFP) and Gag–yellow fluorescent protein (YFP) molecules in whole cells[16–18]. To monitor the assembly of individual particles, we chose the comparatively weak FRET pair of GFP and mCherry[19], precisely because their absorption and emission spectra overlap less than those of CFP and YFP. FRET should therefore be more dependent on the high density of about 5,000 Gag molecules[20] found within a single virion. FRET was detected between Gag–GFP and Gag–mCherry, both within Gag-expressing cells and within individual cell-free VLPs (the FRET is characterized in Supplementary Fig. 4). When single Gag puncta first became visible, the FRET coefficient (the ratio of mCherry to GFP) within them was similar to the FRET coefficient measured in areas containing only diffuse Gag (Fig. 2a). Then, both the GFP and mCherry fluorescence increased, with mCherry fluorescence increasing relatively more rapidly until they reached their maxima synchronously (Fig. 2b, c, and Supplementary Fig. 5). Thus, the FRET in appearing Gag puncta increased 2.5-fold to the level in cell-free VLPs (Fig. 2a). Bleaching the mCherry increased the GFP emission, confirming that FRET occurred in VLPs (Supplementary Fig. 4d). Thus, during the slow emergence, Gag molecules achieve greater proximity, the expected signature of an assembly event, and ultimately are as closely packed as in VLPs released into the extracellular milieu.

The stable fluorescence ultimately achieved by each slowly appearing punctum (Fig. 1b, left) could reflect a steady state in which Gag–GFP is exchanging with the cytoplasmic pool, or it may represent the completion of the assembly of a VLP whose Gag molecules are segregated from the cytoplasmic pool. To distinguish between these possibilities, the puncta were examined with fluorescence recovery after photobleaching (FRAP). This analysis revealed that puncta with a low but rising intensity during the pre-bleach period recovered well during the post-bleach period. Conversely, puncta whose intensity was high and stable during the pre-bleach period did not recover (Fig. 3a, b, and Supplementary Fig. 6). Thus, most puncta recruiting Gag molecules before the bleach continued to recruit new Gag molecules after the bleach; those with steady fluorescence represented puncta in which Gag recruitment was completed and irreversible.

The final step in the genesis of an HIV-1 particle is the fission of virion and cell membranes[21]. At this point, the virion interior should not be able to exchange any molecules—even protons—with the cell cytoplasm. To test whether this final step occurred in the Gag puncta we were observing, we expressed Gag fused to pHluorin[22], a variant of GFP not fluorescent at acidic pH, and then varied the pCO_2 in the medium[23]. Raising the pCO_2 produces acidification as a result of the reaction $CO_2 + H_2O \leftrightarrow H^+ + HCO_3^-$. This should acidify the cytosol more rapidly than the interior of cell-free VLPs as result of the cytosolic enzyme carbonic anhydrase[23]. Thus, increasing the pCO_2 should quench the fluorescence of cytosol-exposed Gag–pHluorin more than Gag–pHluorin in a VLP whose lipid envelope has separated from the cell. As expected, after a brief pulse of higher pCO_2 the fluorescence of the cytosolic-exposed diffuse Gag–pHluorin was quenched more than the Gag–pHluorin in cell-free VLPs (Fig. 3c–f). After the pCO_2 pulse, the fluorescence of the diffuse Gag–pHluorin returned to normal more quickly than that of the isolated VLPs (Fig. 3d). The fluorescence of one population of cell-associated puncta responded indistinguishably from the diffuse Gag to a pulse of pCO_2 (Fig. 3e, f). Conversely, a minority of Gag puncta showed the lower sensitivity to pCO_2 of the budded, cell-free VLPs.

However, 30 min later, most of the cell-associated Gag puncta had shifted to the less pCO_2-sensitive state of the budded VLPs. (Fig. 3e). In addition, after the pulse of pCO_2, the fluorescence of the diffuse Gag and the more pCO_2-responsive population of Gag puncta returned to normal more quickly than the less responsive puncta or the cell-free VLPs (Fig. 3d). Thus, the population of Gag puncta that were as sensitive as diffuse Gag to cytosolic acidification probably consisted of nascent VLPs whose interiors were continuous with the cytosol, whereas the population relatively resistant to pCO_2 probably consisted of budded VLPs. Moreover, when a Gag–pHluorin protein lacking a functional late-budding domain[24] was used to generate puncta, only the pCO_2-sensitive population was seen (Fig. 3f), showing that fission of the VLP and cell membranes was needed to generate pCO_2-resistant (budded) VLPs.

Despite the conclusion that these VLPs have budded and are separate from the cell, they do not move away. This is a confluence of at least two factors. The VLPs are about 100 nm in diameter and their movement is limited by the distance from the cell to the coverslip (20–40 nm). Second, a large fraction of virions remain associated with the cell surface after assembly[11].

We have observed a population of laterally non-motile VLPs that appear over several minutes at the plasma membrane, whose emergence is accompanied by a recruitment of Gag molecules that become progressively closer to each other until they segregate from the cytoplasmic pool and detach from the plasma membrane. These slowly appearing VLPs are not associated with endosomes that approach and retreat from the plasma membrane and represent the vast majority of those that appear at the plasma membrane within the first few hours after Gag expression, particularly in the presence of Vpu. We conclude that this population of slowly appearing puncta represents the genesis of VLPs through *de novo* assembly. Analysis of 370 such assembly events revealed that individual VLPs assembled over an average of 8.5 min, with 5–6 min per VLP being the most frequent rate of assembly (Fig. 4a). Assembly was slower for VLPs that appeared early in the observation period, but accelerated thereafter as Gag concentration increased, stabilizing at 5–6 min (Fig. 4b). Gag concentration influences both the interaction between Gag molecules and the interaction between Gag and the plasma membrane[25] and is very probably a key determinant of assembly kinetics. It is possible that some VLP assembly also takes place on internal membranes that are out of the field of view afforded by TIR-FM, although some previous work argues strongly against this notion[4,5,12]. In examining tens of thousands of VLPs assembling in hundreds of cells, we never observed an organelle reaching the surface and discharging multiple VLPs. Thus, if there is any assembly on internal organelles it does not contribute significantly to the population of VLPs appearing at the basal surface of the cell during the first day of expression or infection.

Altering the expression of Gag–GFP relative to Gag, between ratios of 1:1 and 1:10, did not affect the kinetics of VLP assembly, indicating that their genesis was not influenced by the presence of a GFP tag (Supplementary Fig. 6). Moreover, when Gag was fused to mCherry, which matures more slowly than GFP[26,27], VLPs assembled with

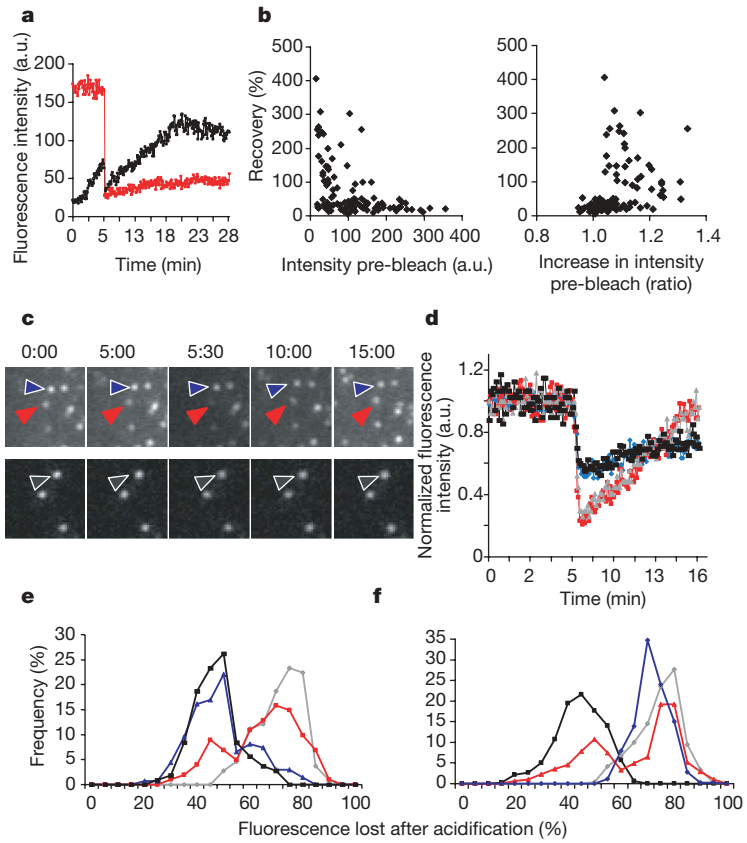

Figure 3 | FRAP analysis of individual Gag puncta. **a**, Plots of Gag–GFP fluorescence intensity over time for the black and red puncta (black and red lines, respectively) shown in Supplementary Fig. 6. **b**, Fluorescence recovery of 100 puncta plotted as a function of either their absolute pre-bleach intensity (left panel) or the fold increase in their intensity before bleaching (right panel) (1 means no increase, more than 1 means increasing). **c**, Images showing Gag–pHluorin puncta before and after the CO_2-mediated acidification. Cells (top panels) or cell-free VLPs (bottom panels) were incubated with pCO_2 for 30 s after 5 min of imaging. The arrows indicate one pCO_2-'sensitive' punctum (red), one pCO_2-'insensitive' punctum (blue) and one cell-free VLP (black). Fields are 3.5 μm × 3.5 μm. Numbers above the fields are minutes:seconds. **d**, Plots of normalized fluorescence intensity over time for the three Gag–pHluorin puncta in **c** (bearing the same colour coding), as well as for a diffuse Gag area (grey). **e**, Loss of fluorescence immediately after pCO_2-mediated acidification for diffuse Gag (grey, $n = 107$), cell-free VLPs (black, $n = 107$) and Gag puncta at $t = 0$ min (red, $n = 101$) and $t = 30$ min (blue, $n = 136$) of imaging. **f**, Loss of fluorescence immediately after pCO_2-mediated acidification of diffuse Gag (grey, $n = 728$), cell-free VLPs (black, $n = 334$), wild-type Gag (red, $n = 308$) and Gag with a late-domain mutation (blue, $n = 366$).

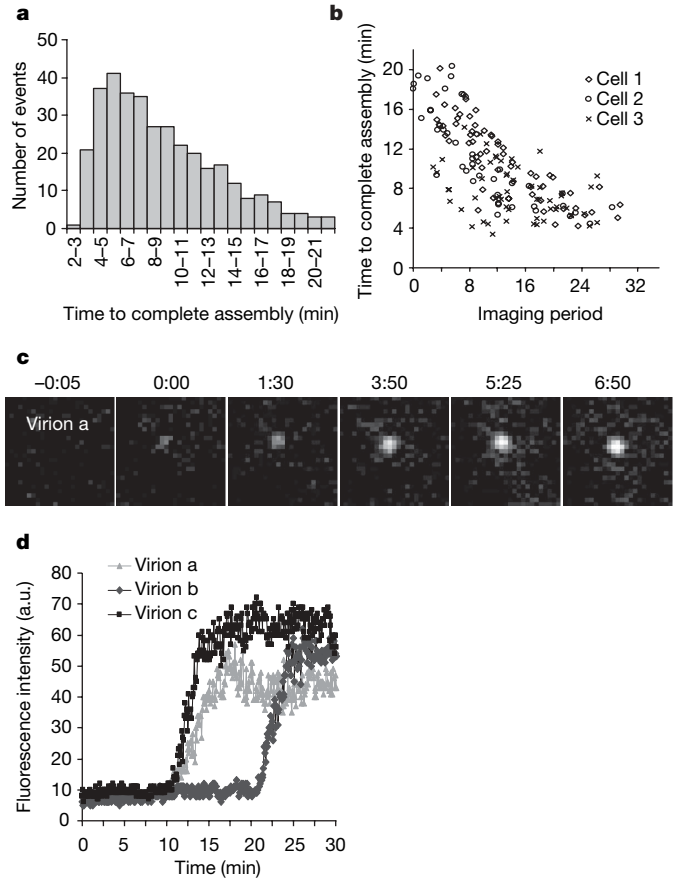

Figure 4 | Variation in HIV-1 assembly kinetics. a, Distribution of the time to complete assembly for 370 individual VLPs in 11 HeLa cells expressing Gag/Gag–GFP. Time to complete assembly was defined as the interval between the points of inflection on plots of fluorescence intensity against time, for each VLP (for example Fig. 1b, c). **b**, Time to complete assembly is plotted against the time at which assembly commenced in three cells imaged for 40 min. Zero time is defined as the time at which observation began; that is, when more than 1 but fewer than 20 VLPs were visible in the TIR field for each cell. $R = -0.71$; $R^2 = 0.5$. **c**, **d**, Assembly of HIV-1 particles from full-length proviral plasmids. **c**, Images of an individual HIV-1 virion assembly event. Fields are 5.5 μm × 5.5 μm. Numbers above the fields are minutes:seconds. **d**, Plots of the fluorescence intensity over time for three assembly events, including that shown in **c**.

kinetics indistinguishable from those containing Gag/Gag–GFP (Supplementary Fig. 7), indicating that the kinetics was not affected by the maturation time of the fluorophore. Significantly, in cells transfected with full-length proviral plasmids in which YFP was inserted into the stalk region of matrix[4] (Supplementary Fig. 8), the assembly of HIV-1 virions was completed with similar kinetics to that of Gag–GFP-containing VLPs (Fig. 4c, d, and Supplementary Fig. 7c). Thus, neither the location nor the nature of the fluorophore linked to Gag, nor the presence of other viral proteins, affected the kinetics of particle assembly.

These studies have allowed the observation and quantitative analysis of the assembly of individual virions in living cells. Elaboration of these approaches should permit characterization of the recruitment of other viral and cellular components to nascent virions and could address many questions that are difficult to tackle with conventional techniques.

METHODS SUMMARY

Expression vectors. Plasmids expressing HIV-1 Gag and Gag–GFP, Vpu–YFP and CD63–Cherry proteins were previously described[4,9], as was an HIV-1 proviral plasmid that carries YFP embedded within Gag[4]. Derivatives were constructed by using standard molecular biology techniques.

Cells and transfection. HeLa cell clones expressing CD63–mCherry or DsRed–clathrin were derived by retroviral transduction. For imaging, cells plated in glass-bottomed dishes were transfected with Lipofectamine2000. VLPs isolated from the supernatant of transfected cells were adhered to polylysine-coated dishes and imaged under the same conditions as VLP-producing cells.

Image acquisition and analysis. Through-the-objective TIR-FM was performed with an inverted Olympus IX-70 microscope with a 60×, 1.45 numerical aperture TIR objective. Imaging of GFP, mCherry or DsRed was achieved by excitation with a 488-nm laser line of an argon laser or a 543-nm HeNe laser, as appropriate. Simultaneous dual-colour imaging was achieved with a dual emission splitter equipped with a 515/30 bandpass filter and a 580lp filter. For FRET analysis, experimentally determined GFP emission bleed-through and direct excitation of mCherry by the 488-nm laser was subtracted from the raw mCherry fluorescence values to yield a corrected mCherry fluorescence that was due to FRET. The FRET coefficient was calculated by dividing the intensity of the corrected mCherry emission by the intensity of the GFP emission in the area of interest. For the analysis of fluorescence recovery, cells were imaged at 5 h after transfection for 5 min, photobleached for 3 min and observed for a further 20 min. During the bleach, the opening of an iris placed in front of the TIR-FM laser was reduced to bleach only a part of the cell. To test the sensitivity of VLPs assembled with Gag–pHluorin to pCO_2, cultures were perfused with 100% CO_2 for 30 s. All image analysis was performed with MetaMorph software.

Received 13 March; accepted 10 April 2008.
Published online 25 May 2008.

1. Brandenburg, B. & Zhuang, X. Virus trafficking—learning from single-virus tracking. *Nature Rev. Microbiol.* **5,** 197–208 (2007).
2. Pelchen-Matthews, A., Kramer, B. & Marsh, M. Infectious HIV-1 assembles in late endosomes in primary macrophages. *J. Cell Biol.* **162,** 443–455 (2003).
3. Sherer, N. M. *et al.* Visualization of retroviral replication in living cells reveals budding into multivesicular bodies. *Traffic* **4,** 785–801 (2003).
4. Jouvenet, N. *et al.* Plasma membrane is the site of productive HIV-1 particle assembly. *PLoS Biol.* **4,** e435 (2006).
5. Welsch, S. *et al.* HIV-1 buds predominantly at the plasma membrane of primary human macrophages. *PLoS Pathogens* **3,** e36 (2007).
6. Gottlinger, H. G. The HIV-1 assembly machine. *AIDS* **15** (Suppl. 5), S13–S20 (2001).
7. Larson, D. R., Johnson, M. C., Webb, W. W. & Vogt, V. M. Visualization of retrovirus budding with correlated light and electron microscopy. *Proc. Natl Acad. Sci. USA* **102,** 15453–15458 (2005).
8. Jaiswal, J. K. & Simon, S. M. Imaging single events at the cell membrane. *Nature Chem. Biol.* **3,** 92–98 (2007).
9. Neil, S. J., Eastman, S. W., Jouvenet, N. & Bieniasz, P. D. HIV-1 Vpu promotes release and prevents endocytosis of nascent retrovirus particles from the plasma membrane. *PLoS Pathogens* **2,** e39 (2006).
10. Neil, S. J., Sandrin, V., Sundquist, W. & Bieniasz, P. D. An interferon-α-induced tethering mechanism inhibits HIV-1 and Ebola virus particle release but is counteracted by the HIV-1 Vpu protein. *Cell Host Microbe* **2,** 193–203 (2007).
11. Neil, S. J., Zang, T. & Bieniasz, P. D. Tetherin inhibits retrovirus release and is antagonized by HIV-1 Vpu. *Nature* **451,** 425–430 (2008).
12. Finzi, A., Orthwein, A., Mercier, J. & Cohen, E. A. Productive human immunodeficiency virus type 1 assembly takes place at the plasma membrane. *J. Virol.* **81,** 7476–7490 (2007).
13. Jaiswal, J. K., Andrews, N. W. & Simon, S. M. Membrane proximal lysosomes are the major vesicles responsible for calcium-dependent exocytosis in nonsecretory cells. *J. Cell Biol.* **159,** 625–635 (2002).
14. Keyel, P. A., Watkins, S. C. & Traub, L. M. Endocytic adaptor molecules reveal an endosomal population of clathrin by total internal reflection fluorescence microscopy. *J. Biol. Chem.* **279,** 13190–13204 (2004).
15. Rappoport, J. Z., Taha, B. W. & Simon, S. M. Movement of plasma-membrane-associated clathrin spots along the microtubule cytoskeleton. *Traffic* **4,** 460–467 (2003).
16. Derdowski, A., Ding, L. & Spearman, P. A novel fluorescence resonance energy transfer assay demonstrates that the human immunodeficiency virus type 1 Pr55Gag I domain mediates Gag–Gag interactions. *J. Virol.* **78,** 1230–1242 (2004).
17. Hubner, W. *et al.* Sequence of human immunodeficiency virus type 1 (HIV-1) Gag localization and oligomerization monitored with live confocal imaging of a replication-competent, fluorescently tagged HIV-1. *J. Virol.* **81,** 12596–12607 (2007).
18. Larson, D. R., Ma, Y. M., Vogt, V. M. & Webb, W. W. Direct measurement of Gag–Gag interaction during retrovirus assembly with FRET and fluorescence correlation spectroscopy. *J. Cell Biol.* **162,** 1233–1244 (2003).
19. Tramier, M., Zahid, M., Mevel, J. C., Masse, M. J. & Coppey-Moisan, M. Sensitivity of CFP/YFP and GFP/mCherry pairs to donor photobleaching on FRET determination by fluorescence lifetime imaging microscopy in living cells. *Microsc. Res. Tech.* **69,** 933–939 (2006).
20. Briggs, J. A. *et al.* The stoichiometry of Gag protein in HIV-1. *Nature Struct. Mol. Biol.* **11,** 672–675 (2004).

21. Pornillos, O., Garrus, J. E. & Sundquist, W. I. Mechanisms of enveloped RNA virus budding. *Trends Cell Biol.* **12,** 569–579 (2002).
22. Miesenbock, G., De Angelis, D. A. & Rothman, J. E. Visualizing secretion and synaptic transmission with pH-sensitive green fluorescent proteins. *Nature* **394,** 192–195 (1998).
23. Simon, S., Roy, D. & Schindler, M. Intracellular pH and the control of multidrug resistance. *Proc. Natl Acad. Sci. USA* **91,** 1128–1132 (1994).
24. Bieniasz, P. D. Late budding domains and host proteins in enveloped virus release. *Virology* **344,** 55–63 (2006).
25. Perez-Caballero, D., Hatziioannou, T., Martin-Serrano, J. & Bieniasz, P. D. Human immunodeficiency virus type 1 matrix inhibits and confers cooperativity on gag precursor–membrane interactions. *J. Virol.* **78,** 9560–9563 (2004).
26. Pedelacq, J. D., Cabantous, S., Tran, T., Terwilliger, T. C. & Waldo, G. S. Engineering and characterization of a superfolder green fluorescent protein. *Nature Biotechnol.* **24,** 79–88 (2006).
27. Shaner, N. C., Steinbach, P. A. & Tsien, R. Y. A guide to choosing fluorescent proteins. *Nature Methods* **2,** 905–909 (2005).

Supplementary Information is linked to the online version of the paper at www.nature.com/nature.

Acknowledgements We thank T. Zang for sharing the HeLa cell line stably expressing DsRed–clathrin light chain; A. Baraff for statistical analysis; members of the Bieniasz and Simon laboratories for discussions; and R. Y. Tsien, T. Kirchhausen and G. Miesenböck for plasmids. This work was supported by grants from the National Institutes of Health (to P.D.B. and S.M.S.) and the National Science Foundation (to S.M.S.). N.J. is supported by an amfAR Mathilde Krim Fellowship in Basic Biomedical Research.

Author Information Reprints and permissions information is available at www.nature.com/reprints. Correspondence and requests for materials should be addressed to P.D.B. (pbienias@adarc.org) or S.M.S. (simon@rockefeller.edu).